nanomaterials

MDPI

Review

Wet-Chemical Preparation of TiO_2-Based Composites with Different Morphologies and Photocatalytic Properties

Liqin Xiang and Xiaopeng Zhao *

Smart Materials Laboratory, Department of Applied Physics, Northwestern Polytechnical University, Xi'an 710129, China; lqxiang@nwpu.edu.cn

* Correspondence: xpzhao@nwpu.edu.cn

Received: 7 September 2017; Accepted: 2 October 2017; Published: 9 October 2017

Abstract: TiO_2-based composites have been paid significant attention in the photocatalysis field. The size, crystallinity and nanomorphology of TiO_2 materials have an important effect on the photocatalytic efficiency. The synthesis and photocatalytic activity of TiO_2-based materials have been widely investigated in past decades. Based on our group's research works on TiO_2 materials, this review introduces several methods for the fabrication of TiO_2, rare-earth-doped TiO_2 and noble-metal-decorated TiO_2 particles with different morphologies. We focused on the preparation and the formation mechanism of TiO_2-based materials with unique structures including spheres, hollow spheres, porous spheres, hollow porous spheres and urchin-like spheres. The photocatalytical activity of urchin-like TiO_2, noble metal nanoparticle-decorated 3D (three-dimensional) urchin-like TiO_2 and bimetallic core/shell nanoparticle-decorated urchin-like hierarchical TiO_2 are briefly discussed.

Keywords: TiO_2-based materials; photocatalysis; nanomorphology; preparation

1. Introduction

Based on its unique chemical and physical characteristics, titanium dioxide (TiO_2) has attracted much attention in many fields including paint pigments, photocatalysis, solar cells, antibacterial agents, electrical energy storage and some advanced functional materials [1–3]. The performance in these applications strongly depends on the microstructure, crystallinity and nanomorphology of TiO_2 [1]. In particular, in the photocatalysis field, although a new type of polymeric photocatalyst—that is, graphitic carbon nitride—has been intensively investigated recently due to its huge advantages—including metal-free contents, visible light absorption ability, suitable band gap for water splitting, stability, and being environmentally benign [4–7]—TiO_2 is still regarded as one of most ideal candidates for photocatalysis because of its strong oxidization, harmlessness to surroundings, chemical inactivity, good stability and low cost [1,3,8,9]. There are three important processes including photo excitation, bulk diffusion and the surface transfer of photoinduced charge carriers in photocatalysis [8]. Thus, the performance of photocatalysis depends strongly upon the charge transfer at the material surface and the light-response range of materials [1,10,11]. The processes of light harvesting and charge transfer efficiencies are affected mainly by the size, crystallinity and nanomorphology of TiO_2 materials [1,8,10–14]. The preparation and photocatalytic properties of TiO_2 with different morphologies including zero-dimensional (micro/nanospheres), one-dimensional (rods, tubes, and nanowires), two-dimensional (films, layers and sheets), and three-dimensional (porous spheres, urchin-like spheres) TiO_2 structures have been widely investigated in the past decade [15–21]. Different ways have been developed for preparing TiO_2 materials with different nanostructures. The general synthesis approaches for the fabrication of TiO_2 materials include sol-gel, hydrothermal

and solvothermal techniques [1]. Controlling the microscopic structures of TiO_2 is still a challenge because TiO_2 precursors are highly reactive.

Pure TiO_2 is not a perfect photocatalyst due to the disadvantages of low photocatalytic efficiency and the narrow light-response region [8]. Doping metal ions or introducing noble metal nanoparticles onto the surface of TiO_2 was demonstrated to be one of the effective ways to enhance the photocatalytic efficiency because these TiO_2-based composites can combine the functions of TiO_2 and metal ions or noble metals [22–25]. Furthermore, the properties of the composites can be adjusted by controlling the ingredients and the microstructures of the TiO_2.

In the past two decades, our group has focused on the synthesis, electrorheological (ER) properties, luminescence properties and photocatalytic activities of TiO_2-based materials [26–32]. A series of TiO_2-based materials with different compositions, crystallinity and interior microstructures have been synthesized by different methods [33–36]. The TiO_2 particles with a familiar microstructure, such as solid spheres [37], hollow spheres [29], porous spheres [28,38], hollow porous spheres [39] and urchin-like spheres [30], were synthesized and characterized in detail. In addition, some TiO_2 composites with a special interior microstructure were also designed and synthesized [40–43]. According to the dielectric design, rare-earth-doped TiO_2 particles were synthesized by sol-gel methods [44–49]. Inspired by the structure of biological surfaces, a kind of composite particle possessing both nano- and micro-scale structures was prepared via a hydrothermal method [50,51]. TiO_2 particles with a cell-like structure were also synthesized [52]. It is noteworthy that the TiO_2-based materials described above show excellent properties in different applications. For example, the rare-earth-doped TiO_2, and the micro- or nano-structured composites with TiO_2 have been demonstrated to show a distinct enhancement in their ER properties [44,50–52]. The hollow Sm^{3+}-doped TiO_2 and the monodisperse mesoporous Eu-doped TiO_2 spheres have shown good luminescent performance [28,29]. The urchin-like TiO_2 and urchin-like TiO_2 decorated with Au, Ag, Co@Au or Co@Ag nanoparticles have shown significant improvement in photocatalytic activities [30–32].

Until now, there have been many review articles introducing the progress made in the field of TiO_2-based materials [1–3,8]. Based on our group's research work on TiO_2 materials, this review is primarily concentrated on the preparation of TiO_2 composites with different morphologies and the photocatalytic activities of urchin-like TiO_2 composites.

2. Preparation of TiO_2 and TiO_2-Based Composites with Different Morphologies

2.1. Micro- and Nano-Spheres

2.1.1. Solid Spheres

Spherical particles with a specific size can be used in many fields, such as photonic crystals, pigments, and so on [15]. In order to obtain monodisperse spherical TiO_2 particles, many methods have been developed. However, it is still a challenge to control the morphology and size of TiO_2 microspheres because of the high reactivity of precursors. Increasing the charge of the particle surface and the steric repulsion of the particles are effective methods of controlling the stability of TiO_2 microspheres [53]. We have reported a simple and reproducible sol-gel method for synthesizing well-defined spherical TiO_2 particles with diameters within 200–800 nm. In this method, polymers including polyethylene glycol (PEG), poly(ethylene oxide)$_{106}$-poly(propylene oxide)$_{70}$-poly(ethylene oxide)$_{106}$ (F127) copolymer, octadecylamine (ODA), and surfactant Span-80 were used to control the size of TiO_2 particles [37]. For example, quasi-monodisperse TiO_2 submicron spheres were synthesized by controlling the hydrolysis of tetrabutyl titanate in ethanol containing the above polymers and small amounts of deionized water. During this process, depending on the used polymer, the transmission time from the transparent solution into white suspension changed from several seconds to minutes. As soon as the transparent solution changed into white suspension, the stirring had to be stopped and the suspension was further aged for 8 h to form quasi-monodisperse TiO_2 submicron spheres.

After high temperature annealing, the spheres were crystallized into the anatase phase. Figure 1 shows the quasi-monodisperse TiO_2 submicron spheres with different diameters within 200–800 nm, synthesized with different polymers.

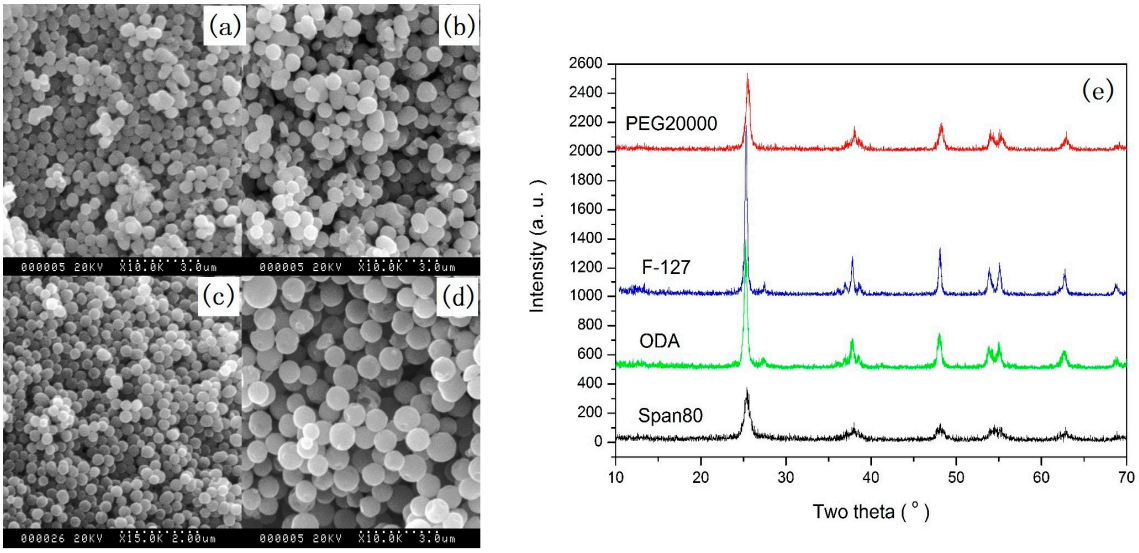

Figure 1. SEM (Scanning electron microscopy) images ((**a**) PEG (polyethylene glycol) 20000, (**b**) ODA (octadecylamine), (**c**) F-127, (**d**) Span80) and the XRD (X-ray diffraction) patterns (**e**) of TiO_2 spheres synthesized by adding different polymers [37].

2.1.2. Hollow Spheres

Due to high specific surface area and low density, hollow structured materials have been widely used in many fields [54]. TiO_2 hollow spheres with a well-defined crystal phase are highly desirable for photocatalysis use [55–57]. Hollow structured TiO_2 can be feasibly synthesized by hard template and soft template methods. Compared to the soft template method, the hard template method is simpler, and so it is frequently used.

An et al. have used polystyrene (PS) spheres as a hard template to prepare hollow Sm^{3+}-doped TiO_2 spheres [29]. The schematic illustration of the formation mechanism is shown in Figure 2. Since the surface of PS spheres obtained by surfactant-free microemulsion polymerization is negatively charged, no additional surface modification of PS spheres is needed for the next coating of TiO_2. In an ethanol/acetonitrile mixed solvent, a small amount of ammonia was used to induce the hydrolysis of tetrobutyl titanate to form the amorphous Sm^{3+}-doped TiO_2 coating layer on the surface of the PS spheres. After washing with ethanol, drying, and annealing, hollow TiO_2:Sm^{3+} spheres, as shown in Figure 3, could be obtained.

Figure 2. Schematic illustration of the formation mechanism for hollow TiO_2:Sm^{3+} spheres [29].

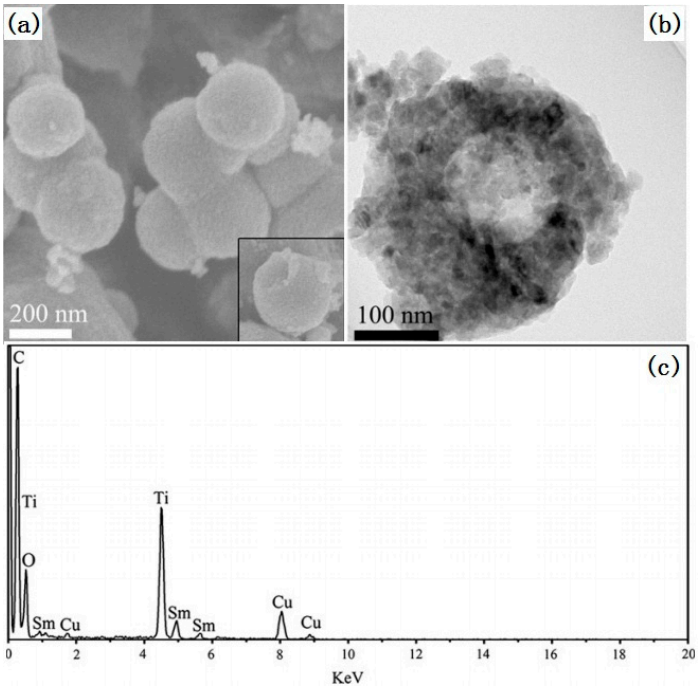

Figure 3. (**a**) SEM image, (**b**) TEM (Transmission Electron Microscopy) image and (**c**) EDS (Energy Dispersive Spectrum) of TiO_2:Sm^{3+} hollow spheres [29].

2.1.3. Porous Spheres

Due to their high surface area, porous materials are very popular for different applications including energy storage, solar cells and catalyzers [58–60]. Mesoporous TiO_2-based materials have attracted much attention for their enhanced reactivity and light harvesting [60]. The macrochannels in mesoporous TiO_2 particles have served as a light-transfer path that can introduce incident photon flux to the interior surface of the TiO_2 particles [58]. A mesoporous structure gives light waves more chances to penetrate deep inside the photocatalyst and more light waves are captured. The crystallinity, pore size and composition are important for tuning the properties of mesoporous TiO_2 spheres [1,8,60]. There has been intensive research concentrated on the design and preparation of porous TiO_2 materials with unique porosities and tunable pore sizes [61–65].

We have synthesized mesoporous Ce-doped TiO_2 spheres by a low-temperature hydrothermal method by using neutral dodecylamine (DDA) as a surfactant and tetrabutyl titanate as a Ti source [64]. To control the rate of hydrolysis of tetrabutyl titanate, a solvent mixture of ethanol and propanol (2:1, v/v) was used. No additional water was used to initialize the hydrolysis and condensation reaction of the tetrabutyl titanate, due to the used $CeCl_3{\cdot}7H_2O$ containing structured water. After the $CeCl_3{\cdot}7H_2O$ was dissolved, the structured water was released. DDA was able to make the solution alkaline and this made it easy to increase the rate of hydrolysis of the tetrabutyl titanate. However, the dissolution of $CeCl_3{\cdot}7H_2O$ also could result in a decrease of the pH value of solution. Thus, $CeCl_3{\cdot}7H_2O$ could service as not only as a dopant but also as an initiator and buffer. After reaction, a precipitate was formed and it was further refluxed for 2 h at 80 °C in an acid solution to get rid of the template and obtain sphere-like mesoporous Ce-doped TiO_2 particles with a diameter of 100–1000 nm as shown in Figure 4. The XRD (X-ray diffraction) patterns in Figure 4 show that the TiO_2 particles are semi-crystalline. The formed anatase crystalline size is very small, about 2–3 nm. In addition, from the TEM (Transmission Electron Microscopy) image, it could be found that the pore structure was worm-like, with a size of 2–3 nm. The Brunauer-Emmett-Teller (BET) surface area of the mesoporous Ce-doped TiO_2 was 118 m^2/g, which is much higher than the 9.6 m^2/g of single-doped TiO_2 obtained without a surfactant.

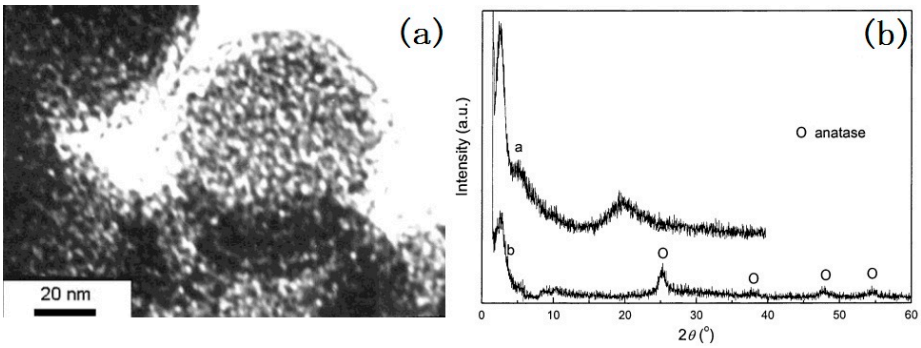

Figure 4. TEM photograph of mesoporous-doped TiO_2 and XRD patterns (**a**) before hydrothermal and acid treatment, (**b**) after hydrothermal and acid treatment of mesoporous-doped TiO_2 [64].

The mesoporous Eu-doped TiO_2 spheres have also been developed by the hydrolysis of tetrabutyl titanate [28]. To increase the thickness of the pore wall, nonionic copolymer Pluronic F-127 was used as a template agent. Europium ethoxide was specially prepared as a doping agent in order to increase the rate of hydrolysis and condensation of the tetrabutyl titanate. Small amounts of water were added to initiate the reaction under stirring. As soon as the solution became slightly white after several minutes, the stirring was stopped. Meanwhile, in order to control the water content, the preparation was conducted under the protection of flowing N_2. After aging for 24–48 h at 35–40 °C, the suspended particles were filtered and washed with ethanol several times. The final products were obtained after calcination at 400 °C for 4 h. The synthesized Eu-doped TiO_2 particles have a spherical morphology and a mesoporous structure, with a pore size of 7–10 nm. The special surface area of the phosphor particles is 158 m^2/g. The high resolution TEM images in Figure 5c show that the pore wall is semi-crystalline that many anatase nanocrystallites are dispersed in the amorphous TiO_2. The XRD patterns showed in Figure 5d have indicated that no peaks corresponding to the europium compound was detected and no shift of the anatase peaks was observed after doping with Eu^{3+}. It can be concluded that Eu^{3+} ions are mainly dispersed in the amorphous TiO_2 region.

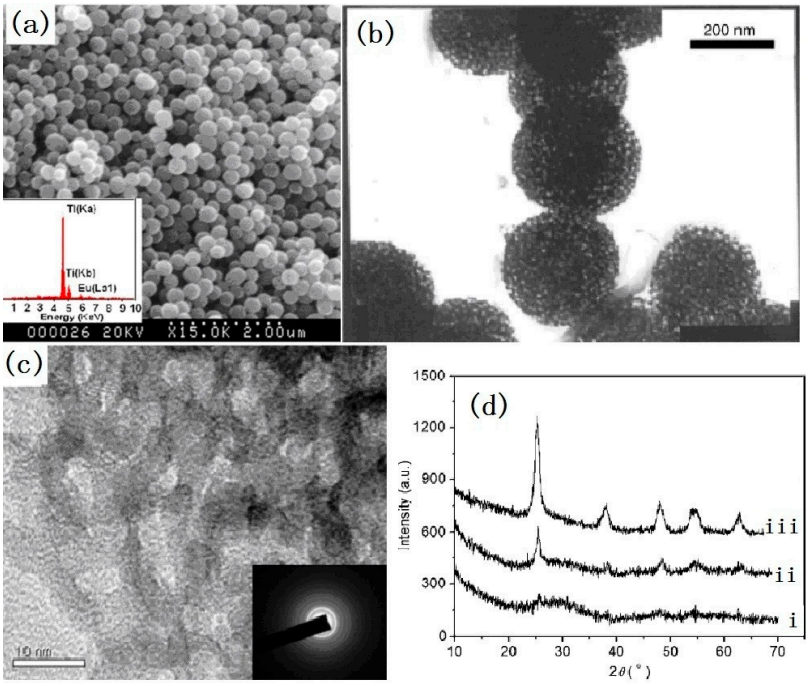

Figure 5. (**a**) SEM image and EDS spectra, (**b**) TEM image, (**c**) high resolution TEM image and corresponding electron diffraction pattern of monodisperse mesoporous after 400 °C calcinations, (**d**) XRD patterns: (i) before calcinations, (ii) after 400 °C calcinations, and (iii) after 500 °C calcinations [28].

2.1.4. Hollow and Porous Spheres

Compared to single hollow spheres, hollow TiO_2 spheres with a porous shell are more interesting in photocatalysis because they can provide a higher surface area and active site points, decreased diffusion resistance, and increased accessibility to reactants [66]. Several methods have been reported to synthesize hollow TiO_2 spheres with a porous shell [66,67]. Among these methods, the template method is the most popular. Different sacrificial templates can be used for controlling the size and morphology of such a hollow nanostructure. The template method followed by a hydrothermal or calcination treatment is often used to synthesize hollow TiO_2 spheres with a crystalline shell [39]. Figure 6 shows a typical process of preparing hollow TiO_2 spheres with a crystalline shell. In this process, amorphous TiO_2 was firstly coated onto the surface of SiO_2 spheres by the sol-gel method in an alkaline solution. Then, the composite microspheres were subjected to a hydrothermal or calcination treatment. Meanwhile, the amorphous TiO_2 was crystallized into nanocrystals and the mesoporous structure was formed by nanocrystal stacking. Finally, the SiO_2 core was removed by etching in an alkaline solution. As shown in Figure 7, the sample prepared by hydrothermal treatment had a mean diameter of 620 nm with a 180 nm thick mesoporous TiO_2 shell. The BET surface area was 231.1 m^2/g and the pore size was 6.5 nm. However, the sample prepared by calcination had a mean diameter of 440 nm with a 90 nm thick mesoporous TiO_2 shell. The BET surface area was 158.3 m^2/g.

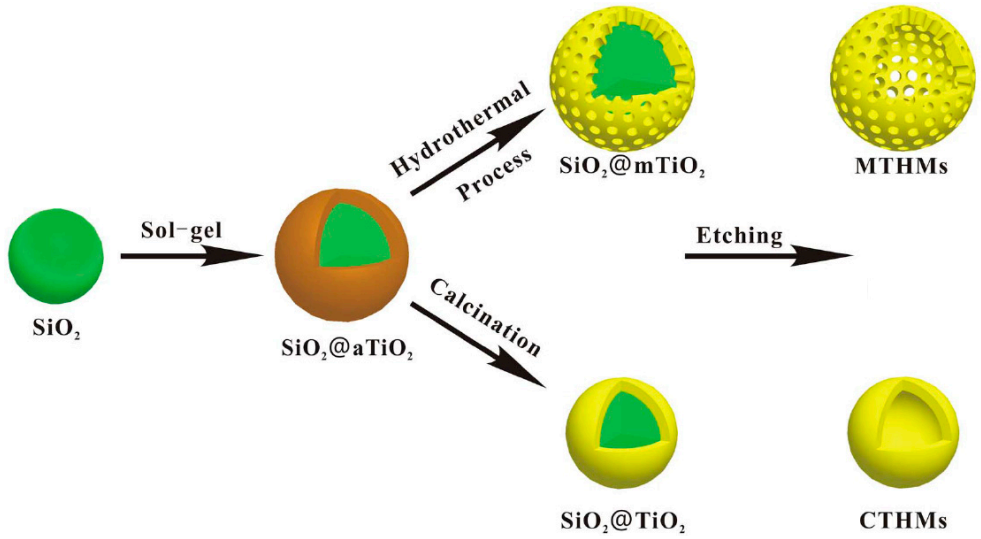

Figure 6. Schematic illustration of the process for the fabrication of the mesoporous TiO_2 hollow microspheres [39].

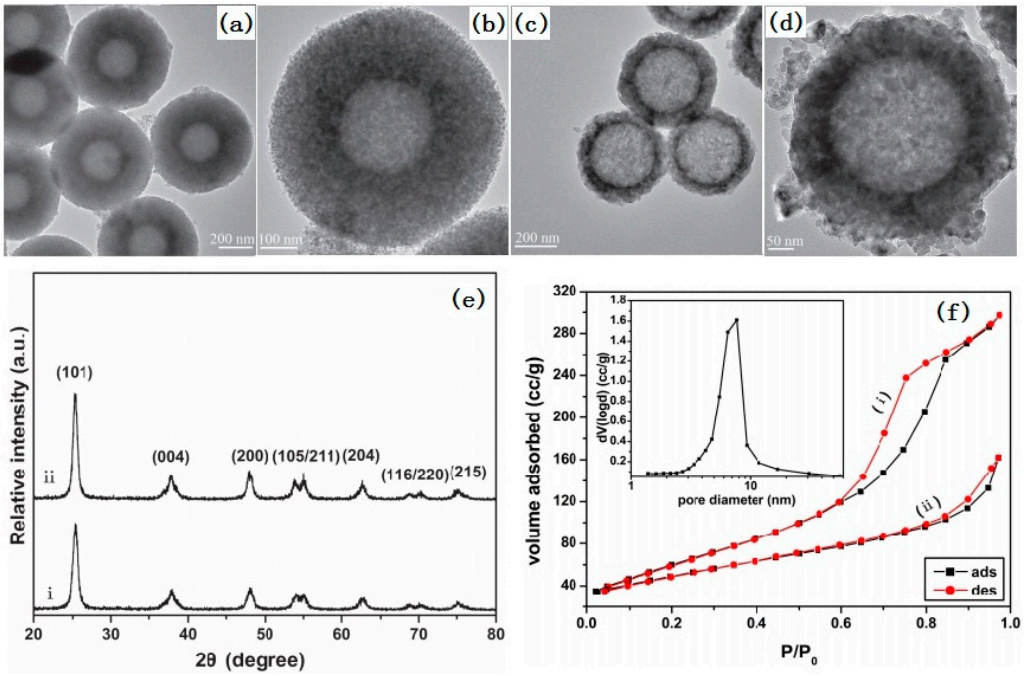

Figure 7. TEM images (**a**,**b**), XRD patterns (**e**-i) and nitrogen adsorption-desorption isotherms (**f**-i) of the sample prepared by the hydrothermal process; TEM images (**c**,**d**), XRD patterns (**e**-ii) and nitrogen adsorption-desorption isotherms (**f**-ii) of the sample prepared by the calcination process [39].

2.2. 3D Urchin-Like Hierarchical Particles

Urchin-like microspheres possess an epitaxial multilevel structure. The unique micro/nano hierarchical structure has two obvious advantages over single nano-scale or micro-scale structures when they are used as photocatalysts [54,68]. One is that urchin-like TiO_2 is more efficient at absorbing incidental light because of the increase of multiple-reflection of the hierarchical microspheres [54]. The other is that urchin-like hierarchical TiO_2 is easy to separate from waste water by the filtration or sedimentation methods. The template-assisted method is a familiar approach to prepare the hierarchical materials. However, it is troublesome to remove templates from products. Impurities are easily introduced into products in the process of utilization and removal of templates. The template-free method is accepted as an ideal strategy which can overcome the drawbacks. Recently, TiO_2 particles with different hierarchical structures have been successfully fabricated via the template-free method [69–73].

2.2.1. Urchin-Like Hierarchical TiO_2 Particles

We have developed a synthesis of a kind of 3D urchin-like TiO_2 microspheres via a solvothermal method without adding any surfactant or template [30]. Tetrabutyl titanate and titanium tetrachloride ($TiCl_4$) aqueous solution were used as the reactant, and toluene was used as the solvent. The solvothermal reaction took place in a Teflon-lined autoclave at 150 °C for 24 h. Sea-urchin-like 3D hierarchical TiO_2 microspheres with a uniform size of 2.5–3.0 μm were obtained (Figure 8). The 3D hierarchical microspheres were made of single crystalline rutile nanoneedles with diameters about 20–40 nm, which grew radially from the core of the microspheres. The morphology and crystal phase of the 3D hierarchical TiO_2 microspheres could be influenced by some factors, such as the ratio of tetrabutyl titanate to $TiCl_4$, the solvothermal temperature, and so on. By tracing the particle morphology change by SEM and XRD techniques, we concluded that the formation of 3D hierarchical TiO_2 microspheres mainly concerned three steps, i.e., nucleation, self-assembly, dissolution and recrystallization, as depicted in Figure 9. In the nucleation stage, nanoparticles were formed. Then,

the nanoparticles assembled into microspheres. Finally, the microspheres gradually changed into the urchin-like hierarchical structure by dissolution and recrystallization.

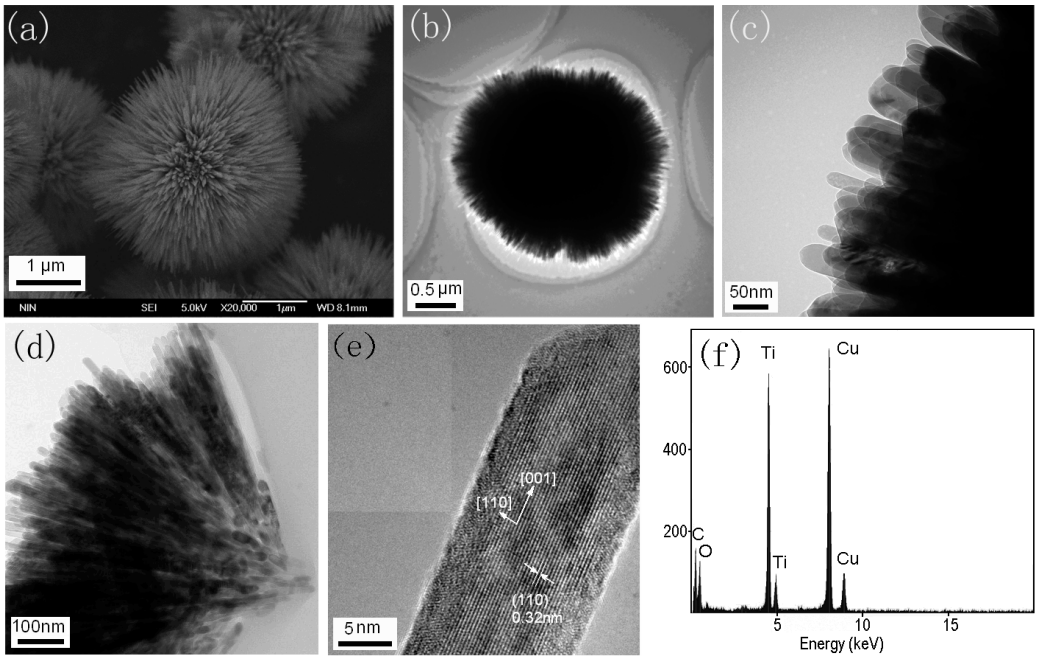

Figure 8. SEM image (**a**), TEM images (**b**–**e**), and EDS (**f**) of the urchin-like hierarchical TiO_2 [30].

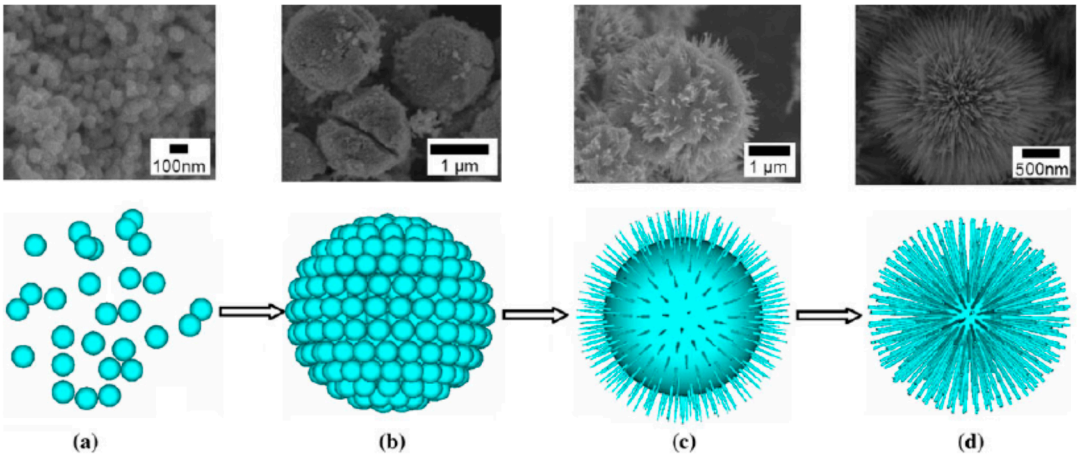

Figure 9. Schematic illustration of the formation process of 3D urchin-like hierarchical TiO_2: (**a**) nanoparticle; (**b**) microsphere; (**c**) similar urchin-like sphere; (**d**) urchin-like sphere [30].

2.2.2. Cr Doped Urchin-Like Hierarchical TiO_2 Particles

Urchin-like Cr-doped TiO_2 particles could be also synthesized by the same solvothermal method described above in a solution of titanium tetrabutyl titanate dissolving $CrCl_3$ [73]. The morphology of Cr-doped TiO_2 particles is characterized by SEM images shown in Figure 10. The mean particle size of the hierarchical microspheres can be adjusted within 1–5 μm and the diameter of the nanorods is about 20–30 nm. The EDS results showed that the content of the Cr element in the Cr-doped TiO_2 particles was ~2.9 mol %.

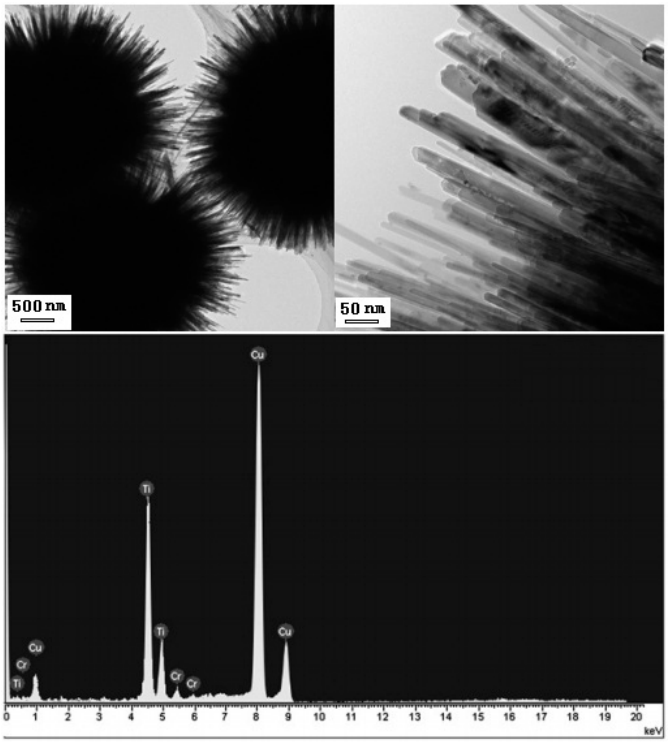

Figure 10. TEM images and EDS spectra of Cr-doped urchin-like TiO2 particles [73].

2.2.3. Noble Metal Nanoparticle-Decorated 3D Urchin-Like TiO_2 Particles

Noble metal nanoparticle-decorated semiconductors are interesting for photocatalysis because of their combined properties [74]. Decorating the noble metal nanoparticles (e.g., Au, Ag and Pt) onto the surface of TiO_2 is an effective method to improve the photocatalytic activity because not only light-harvesting efficiency can be enhanced due to the surface plasmon resonance of noble metal nanoparticles, but the recombination of surface radicals can also be slowed down by capturing photogenerated electrons of noble metal nanoparticles [75–79]. Figure 11 shows a schematic illustration of 3D urchin-like hierarchical TiO_2 microspheres decorated with Au nanoparticles via a two-step wet-chemical process [31]. In the first step, the surface of the urchin-like TiO_2 microspheres was modified with APTES (3-aminopropyl-triethoxysilane) that possess amidocyanogen. Then, the modified particles were decorated with Au nanoparticles in $HAuCl_4$ aqueous solution by the reduction of $NaBH_4$. Since the amidocyanogen could interact with Au nanoparticles by a weak covalent bond, Au nanoparticles were closely attached to the surface of the TiO_2 nanostructures, as shown in Figure 12. It was seen that the Au nanoparticles with diameters of about 2–10 nm mainly adhered to the surface of the needles uniformly. Most of the Au nanoparticles possess a rhombic dodecahedra structure. The UV-Vis (ultraviolet-visible) spectra show an absorption band located at the wavelength of about 530 nm due to the surface plasmon resonance of Au nanoparticles.

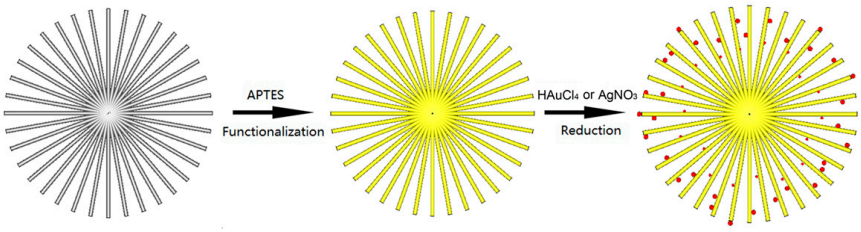

Figure 11. Schematic illustration of the synthesis process of urchin-like TiO_2 decorated with Au or Ag nanoparticles [31].

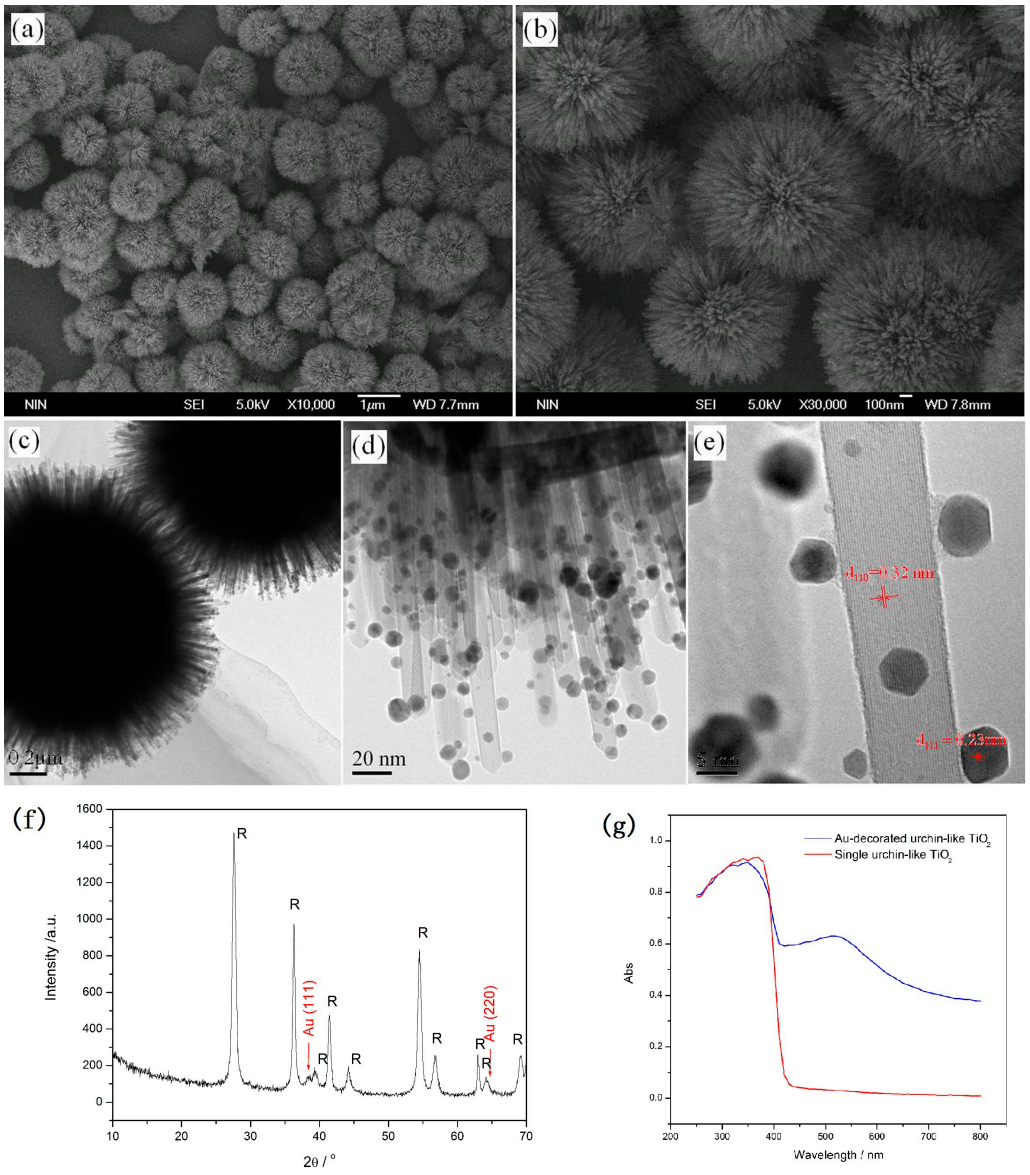

Figure 12. SEM images (**a**,**b**), TEM images (**c**–**e**), XRD pattern (**f**) and UV-Vis absorption spectra (**g**) of Au-decorated 3D urchin-like TiO_2 nanostructures [31].

The urchin-like TiO_2 microspheres decorated with Ag nanoparticles could be also prepared by the similar process. As shown in Figure 13, the Ag nanoparticles with diameters of about 2 nm are decorated on the TiO_2 nanoneedles homogeneously. A broad absorption band at around 500 nm, corresponding to the surface plasmon resonance of the Ag nanoparticles, appears in the UV-Vis absorption spectrum (Figure 13f).

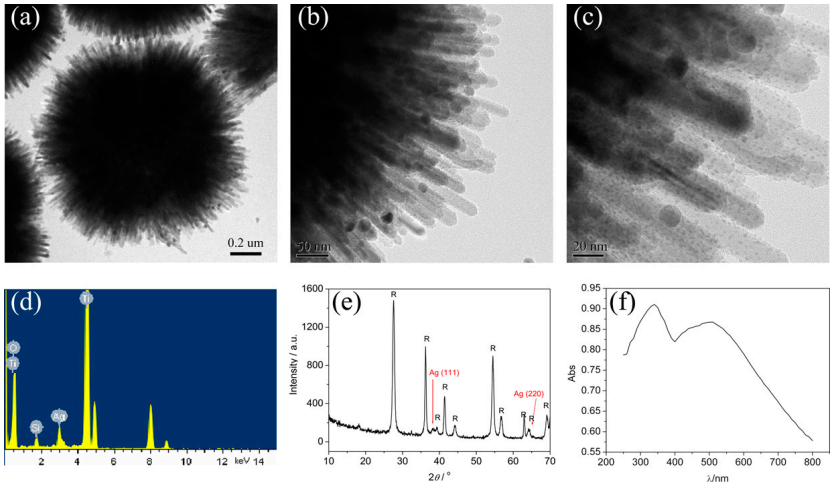

Figure 13. TEM images (**a**–**c**), EDS (**d**), XRD (**e**), and UV-Vis absorption spectrum (**f**) of Ag-decorated 3D urchin-like TiO_2 nanostructures [31].

2.2.4. Core/Shell-Structured Bimetallic Nanoparticle-Decorated 3D Urchin-Like Hierarchical TiO_2 Particles

Bimetallic nanostructures often show a more excellent comprehensive performance over their monometallic counterpart [80]. Especially core/shell bimetallic nanostructures with a magnetic core and a noble-metallic shell have aroused researchers' interest [81–85]. The magnetic core can offer a drive force for the recycling of samples, while the noble-metal shell can improve the optical properties [85]. Figure 14 shows a typical preparation process of a kind of 3D urchin-like hierarchical TiO_2 decorated with a bimetallic core/shell nanoparticle (Co@Au and Co@Ag). The preparation includes three steps, i.e., surface activation, electroless plating and in-situ replacement [32]. First, the surface of the urchin-like TiO_2 microspheres was activated by implanting Pd nanodots. Then, Co nanoparticles were formed and adhered to the nanoneedle surface of the urchin-like TiO_2 microspheres by electroless plating. Finally, Ag or Au were further formed and coated on the surface of the Co nanoparticles by an in-situ replacement process.

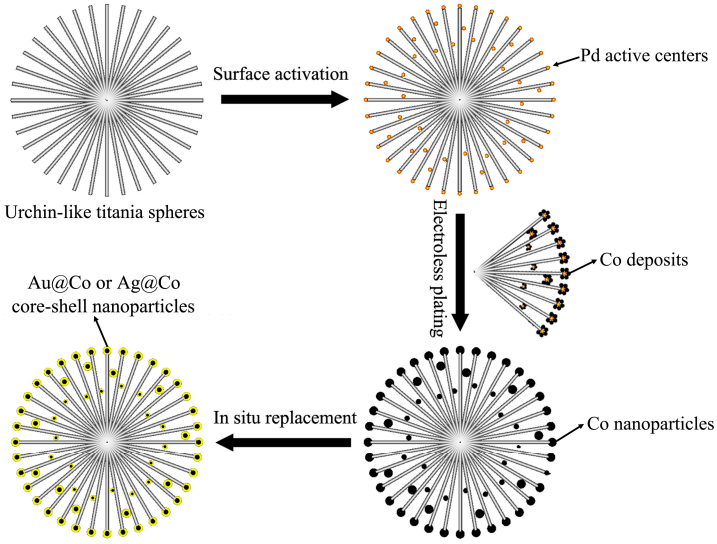

Figure 14. A schematic synthesis process of urchin-like TiO_2 decorated with core/shell-structured Co@Au or Co@Ag bimetallic nanoparticles [32].

The SEM and TEM images in Figure 15 show the morphology of Co@Au/TiO_2 composites. It can be seen that many core/shell nanostructured nanoparticles with diameters of 10–80 nm are attached to the surface of TiO_2 nanorods. The images of the elemental mapping of core/shell nanoparticles further identify that the core is Co and the shell is Au. The size and distribution of the bimetallic particles can be adjusted by controlling the ratio of Co to TiO_2 during the electroless plating process. The thickness of the Au or Ag shell could be controlled by adjusting the concentration of $HAuCl_4$ or $AgNO_3$ in the solution and the reaction time. Both the Co@Au/TiO_2 and Co@Ag/TiO_2 particles showed good response to an applied external magnetic field [32].

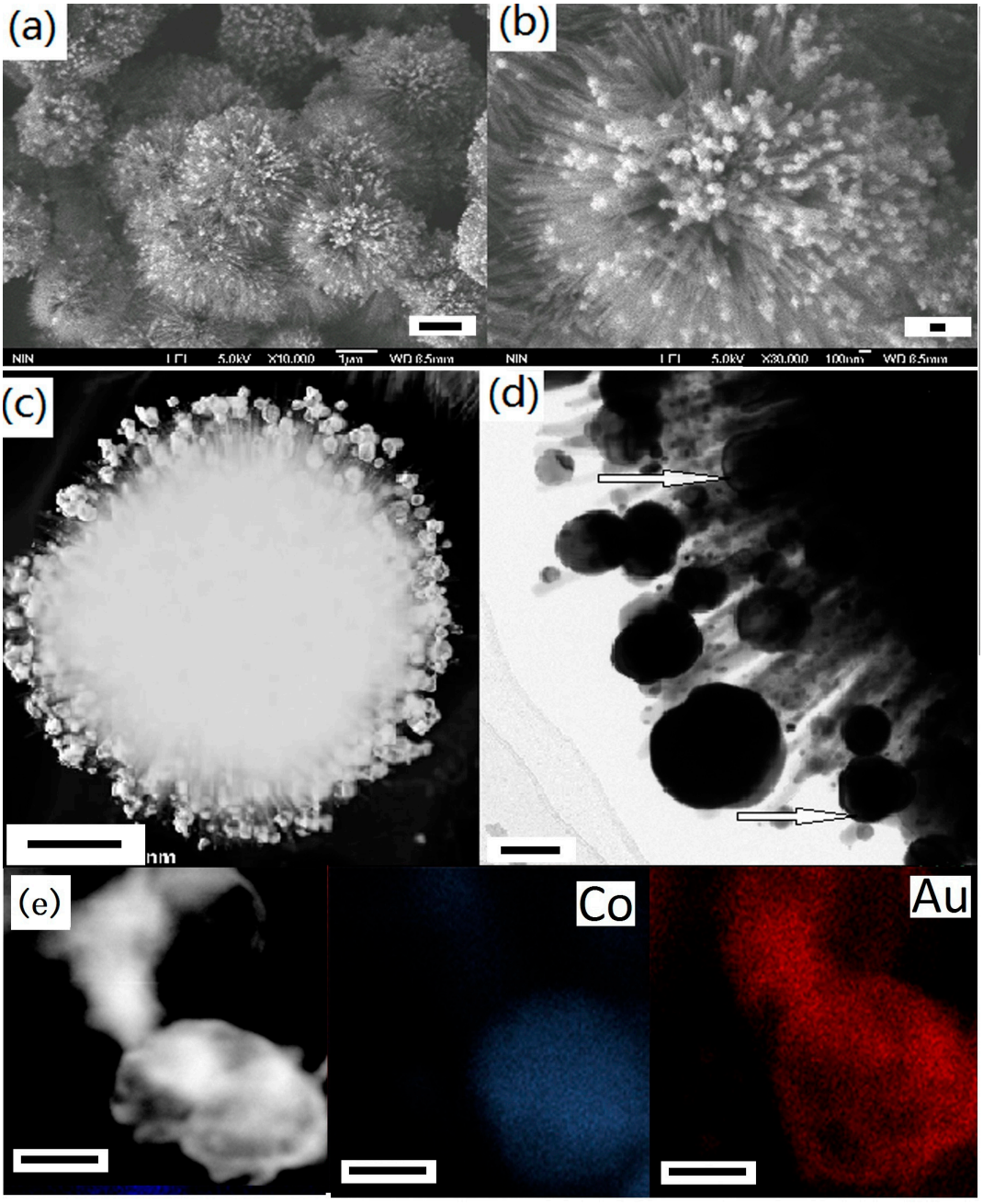

Figure 15. The SEM and TEM images of Co@Au/TiO_2 composites: (**a**,**b**) SEM images, (**c**,**d**) TEM images, (**e**) high-resolution TEM images; (**e**) the local elemental mapping of Co and Au (Scale bar = 1 μm for (**a**); scale bar = 100 nm for (**b**); scale bar = 500 nm for (**c**); scale bar = 100 nm for (**d**); scale bar = 50 nm for (**e**)) [32].

2.2.5. Photocatalytic Activity of Urchin-Like Hierarchical TiO_2 and Their Composites

Although TiO_2 is an ideal candidate for photocatalysis because of its strong oxidization, harmlessness to surroundings, chemical inactivity, good stability and low cost, the main weakness of TiO_2 is the lack of visible light response due to the large band gap. Therefore, the question of how to increase the efficiency of visible light harvesting is an important research topic in this field [1]. Although single controlling the morphology of TiO_2 materials cannot increase the efficiency of visible light harvesting, it is possible to enhance the visible light harvesting of TiO_2 composites by combining ion doping or noble metal decoration with morphology control. Ion doping or noble metal decoration can induce or increase the visible light absorption of TiO_2, while the absorption effect can be further enhanced by other effects from material morphology, such as decreased light scattering or increased multiple reflection, etc.

The photocatalytic efficiency of commercial P25, urchin-like TiO_2 and Au or Ag-decorated urchin-like TiO_2 was evaluated by degrading MB (methyl blue) under UV-Vis light irradiation. It was found that the photocatalytic degradation efficiency under the same conditions followed the order: Ag/TiO_2 > Au/TiO_2 > TiO_2 > P25 (Figure 16). By the photoluminescence spectra, Au or Ag nanoparticles decorated on the surface of TiO_2 were demonstrated to be able to effectively capture photogenerated electrons and prevent electron/hole recombining (Figure 16). In addition, the urchin-like micro/nano hierarchical structure also may increase the visible light harvesting efficiency by the multiple-reflection of nanoneedles. These should be responsible for the enhanced photocatalytic efficiency of urchin-like TiO_2 microspheres after decoration with Au or Ag nanoparticles. Similarly, the light-harvesting efficiency could also be enhanced by decorating with Co@Au or Co@Ag bimetallic nanoparticles, as shown in Figure 17. As a result, the photocatalytical efficiency of urchin-like TiO_2 was enhanced obviously, as shown in Figure 17, by the experiment of decolorizing methyl blue (MB) solution.

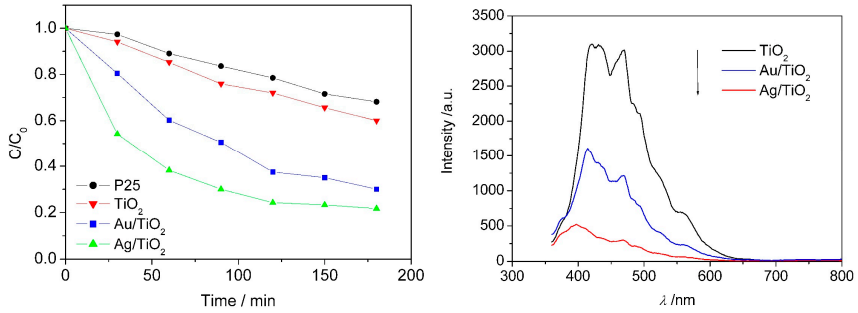

Figure 16. Photodegradation curves of MB (methyl blue) in the presence of P25, TiO_2, Au/TiO_2 and Ag/TiO_2 (**left**); Photoluminence spectra (λ_{ex} = 215 nm) of pure urchin-like TiO_2, Au/TiO_2 and Ag/TiO_2 (**right**) [31].

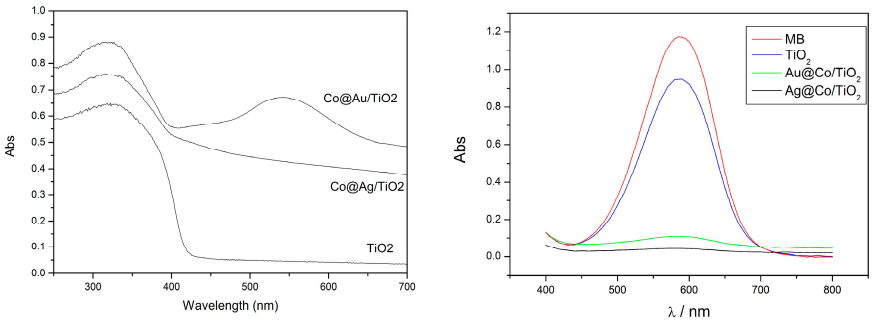

Figure 17. UV-Vis absorption spectra of TiO_2, $Co@Au/TiO_2$ and $Co@Ag/TiO_2$ (**left**); UV-Vis absorption spectra of MB before and after degradation with TiO_2, $Co@Au/TiO_2$ and $Co@Ag/TiO_2$ for 15 min at room temperature (**right**) [32].

3. Summary

Based on our group's research work, we provided a brief review of the synthesis of TiO_2 with different morphologies and the photocatalytic properties of urchin-like TiO_2, noble metal nanoparticle-decorated 3D urchin-like TiO_2 and core/shell-structured bimetallic nanoparticle-decorated 3D urchin-like hierarchical TiO_2. The examples of the fabrication of solid spheres, hollow spheres, porous spheres, and porous and hollow microspheres of anatase TiO_2-based materials were introduced. The synthesis and photocatalytic efficiency of urchin-like rutile TiO_2, urchin-like rutile TiO_2 nanostructures decorated with Au or Ag nanoparticles and core/shell-structured bimetallic nanoparticles (Co@Au and Co@Ag) were especially introduced. The results of photocatalytic tests show that 3D urchin-like hierarchical structures have unique merits in the efficient harvesting of solar light, and decorating Au, Ag or bimetallic nanoparticles on the surface of 3D urchin-like TiO_2 can promote photoinduced charge-carrier separation.

Acknowledgments: This work was supported by the National Natural Science Foundation of China (Grant Nos. 51502247 and 11674267)

Author Contributions: Liqin Xiang and Xiaopeng Zhao wrote the paper.

Conflicts of Interest: The authors declare no conflict of interest.

References

1. Fattakhova-Rohlfing, D.; Zaleska, A.; Bein, T. Three-Dimensional Titanium Dioxide Nanomaterials. *Chem. Rev.* **2014**, *114*, 9487–9558. [CrossRef] [PubMed]
2. Abdullah, N.; Kamarudin, S.K. Titanium dioxide in fuel cell technology: An overview. *J. Power Sources* **2015**, *278*, 109–118. [CrossRef]
3. Chen, X.B.; Mao, S.S. Titanium dioxide nanomaterials: Synthesis, properties, modifications, and applications. *Chem. Rev.* **2007**, *107*, 2891–2959. [CrossRef] [PubMed]
4. Zhang, G.; Lan, Z.A.; Wang, X. Conjugated Polymers: Catalysts for Photocatalytic Hydrogen Evolution. *Angew. Chem. Int. Ed.* **2016**, *55*, 15712–15727. [CrossRef] [PubMed]
5. Kessler, F.K.; Zheng, Y.; Schwarz, D.; Merschjann, C.; Schnick, W.; Wang, X.; Bojdys, M.J. Functional carbon nitride materials-design strategies for electrochemical devices. *Nat. Rev. Mater.* **2017**, *2*, 17030. [CrossRef]
6. Zhang, G.; Lan, Z.A.; Wang, X. Surface engineering of graphitic carbon nitride polymers with cocatalysts for photocatalytic overall water splitting. *Chem. Sci.* **2017**, *8*, 5261–5274. [CrossRef] [PubMed]
7. Ong, W.J.; Tan, L.L.; Ng, Y.H.; Yong, S.T.; Chai, S.P. Graphitic carbon nitride (g-C_3N_4)-based photocatalysts for artificial photosynthesis and environmental remediation: Are we a step closer to achieving sustainability? *Chem. Rev.* **2016**, *116*, 7159–7329. [CrossRef] [PubMed]
8. Liu, G.; Wang, L.; Yang, H.G.; Cheng, H.M.; Lu, G.Q. TiO_2-based photocatalysts-crystal growth, doping and heterostructuring. *J. Mater. Chem.* **2010**, *20*, 831–843. [CrossRef]
9. Ruokolainen, M.; Ollikainen, E.; Sikanen, T.; Kotiaho, T.; Kostiainen, R. Oxidation of tyrosine-phosphopeptides by titanium dioxide photocatalysis. *J. Am. Chem. Soc.* **2016**, *138*, 7452–7455. [CrossRef] [PubMed]
10. Kisch, H. Semiconductor photocatalysis-mechanistic and synthetic aspects. *Angew. Chem. Int. Ed.* **2013**, *52*, 812–847. [CrossRef] [PubMed]
11. Du, J.; Lai, X.; Yang, N.; Zhai, J.; Kisailus, D.; Su, F.; Wang, D.; Jiang, L. Hierarchically Ordered Macro-Mesoporous TiO_2-Graphene Composite Films: Improved Mass Transfer, Reduced Charge Recombination, and Their Enhanced Photocatalytic Activities. *ACS Nano* **2011**, *5*, 590–596. [CrossRef] [PubMed]
12. Li, Y.F.; Liu, Z.P. Particle size, shape and activity for photocatalysis on TiO_2 anatase nanoparticles in aqueous surroundings. *J. Am. Chem. Soc.* **2011**, *133*, 15743–15752. [CrossRef] [PubMed]
13. Meulen, T.; Mattson, A.; Oesterlund, L. A comparative study of the photocatalytic oxidation of propane on anatase, rutile, and mixed-phase anatase-rutile TiO_2 nanoparticles: Role of surface intermediates. *J. Catal.* **2007**, *25*, 131–138.
14. Kang, X.W.; Chen, S.W. Photocatalytic reduction of methylene blue by TiO_2 nanotube arrays: Effects of TiO_2 crystalline phase. *J. Mater. Sci.* **2010**, *45*, 2696–2702. [CrossRef]

15. Tanaka, S.; Nogami, D.; Tsuda, N.; Miyake, Y. Synthesis of highly-monodisperse spherical TiO_2 particles with diameters in the submicron range. *J. Colloid Interface Sci.* **2009**, *334*, 188–194. [CrossRef] [PubMed]
16. Momeni, M.; Ghayeb, Y. Fabrication, characterization and photoelectrochemical performance of chromium-sensitized TiO_2 nanotubes as efficient photoanodes for solar water splitting. *J. Solid State Electrochem.* **2016**, *20*, 683–689. [CrossRef]
17. Ghicov, A.; Schmuki, P. Self-ordering electrochemistry: A review on growth and functionality of TiO_2 nanotubes and other self-aligned MO_x structures. *Chem. Commun.* **2009**, 2791–2808. [CrossRef] [PubMed]
18. Zhang, J.; Zhu, Z.; Tang, Y.; Müllen, K.; Feng, X. TiO_2 Nanosheet-Mediated Construction of a Two-Dimensional TiO_2/Cadmium Sulfide Heterostructure for High Hydrogen Evolution Activity. *Adv. Mater.* **2014**, *26*, 734–738. [CrossRef] [PubMed]
19. Bartl, M.H.; Boettcher, S.W.; Frindell, K.L.; Stucky, G.D. 3-D molecular assembly of function in TiO_2-based composite material systems. *Acc. Chem. Res.* **2005**, *38*, 263–271. [CrossRef] [PubMed]
20. Zhu, T.; Li, J.; Wu, Q. Construction of TiO_2 hierarchical nanostructures from nanocrystals and their photocatalytic properties. *ACS Appl. Mater. Interfaces* **2011**, *3*, 3448–3453. [CrossRef] [PubMed]
21. Li, H.; Bian, Z.; Zhu, J.; Zhang, D.; Li, G.; Huo, Y.; Li, H.; Lu, Y. Mesoporous TiO_2 spheres with tunable chamber lasmon and enhanced photocatalytic activity. *J. Am. Chem. Soc.* **2007**, *129*, 8406–8407. [CrossRef] [PubMed]
22. Choi, W.; Termin, A.; Hoffman, M.R. The role of metal ion dopants in quantum-sized TiO_2: Correlation between photoreactivity and charge carrier recombination dynamics. *J. Phys. Chem.* **1994**, *98*, 13669–13679. [CrossRef]
23. Su, R.; Tiruvalam, R.; He, Q.; Dimitratos, N.; Kesavan, L.; Hammond, C.; Lopez-Sanchez, J.A.; Bechstein, R.; Kiely, C.J.; Hutchings, G.J.; et al. Promotion of phenol photodecomposition over TiO_2 using Au, Pd, and AuPd nanoparticles. *ACS Nano* **2012**, *6*, 6284–6292. [CrossRef] [PubMed]
24. Smirnova, N.; Vorobets, V.; Linnik, O.; Manuilov, E.; Kolbasovb, G.; Eremenkoa, A. Photoelectrochemical and photocatalytic properties of mesoporous TiO_2 films modified with silver and gold nanoparticles. *Surf. Interface Anal.* **2010**, *42*, 1205–1208. [CrossRef]
25. Arabtzis, I.M.; Stergiopoulos, T.; Andreeva, D.; Kitova, S.; Neophytides, S.G.; Falaras, P. Charaterizarion and photocatalytic activity of Au/TiO_2 thin films for azo-dye degradation. *J. Catal.* **2003**, *220*, 127–135. [CrossRef]
26. Yin, J.B.; Zhao, X.P. Preparation and Enhanced Electrorheological Activity of TiO_2 Doped with Chromium Ion. *Chem. Mater.* **2004**, *16*, 321–328. [CrossRef]
27. Zhao, X.P.; Duan, X. In situ sol-gel preparation of polysaccharide/titanium oxide hybrid colloids and their electrorheological effect. *J. Colloid Interface Sci.* **2002**, *251*, 376–380. [CrossRef] [PubMed]
28. Yin, J.B.; Xiang, L.Q.; Zhao, X.P. Monodisperse spherical mesoporous Eu-doped TiO_2 phosphor particles and the luminescence properties. *Appl. Phys. Lett.* **2007**, *90*, 113112. [CrossRef]
29. An, G.F.; Yang, C.S.; Jin, S.H.; Chen, G.W.; Zhao, X.P. Hollow TiO_2:Sm^{3+} spheres with enhanced photoluminescence fabricated by a facile method using polystyrene as template. *J. Mater. Sci.* **2013**, *48*, 5483–5488. [CrossRef]
30. Xiang, L.Q.; Zhao, X.P.; Yin, J.B.; Fan, B.L. Well-organized 3-D urchin-like multilevel TiO_2 microspheres with high photocatalytic activity. *J. Mater. Sci.* **2012**, *47*, 1436–1445. [CrossRef]
31. Xiang, L.Q.; Zhao, X.P.; Shang, C.H.; Yin, J.B. Au or Ag nanoparticle-decorated 3D urchin-like TiO_2 nanostructures: Synthesis, characterization, and enhanced photocatalytic activity. *J. Colloid Interface Sci.* **2013**, *403*, 22–28. [CrossRef] [PubMed]
32. Xiang, L.Q.; Liu, S.; Yin, J.B.; Zhao, X.P. Bimetallic core/shell nanoparticle-decorated 3D urchin-like hierarchical TiO_2 nanostructures with magneto-responsive and decolorization characteristics. *Nanoscale Res. Lett.* **2015**, *10*, 84. [CrossRef] [PubMed]
33. Yin, J.B.; Zhao, X.P. Titanate nano-whisker electrorheological fluid with high suspended stability and ER activity. *Nanotechnology* **2006**, *17*, 192–196. [CrossRef]
34. Guo, H.X.; Zhao, X.P.; Ning, G.H.; Liu, G.Q. Synthesis of Ni/Polystyrene/TiO_2 multiply coated microsphere. *Langmuir* **2003**, *19*, 4884–4888. [CrossRef]
35. Guo, H.X.; Zhao, X.P.; Guo, H.L.; Zhao, Q. Preparation of porous SiO_2/Ni/TiO_2 multiply microsphere responsive to electric and magnetic fields. *Langmuir* **2003**, *19*, 9799–9803. [CrossRef]
36. Yin, J.B.; Zhao, X.P. Electrorheological fluids based on glycerol-activated TiO_2 gel and silicone oil with high yield strength. *J. Colloid Interface Sci.* **2003**, *257*, 228–236. [CrossRef]

37. Xiang, L.Q.; Yin, J.B.; Gao, W.S.; Zhao, X.P. Controllable Preparation of Quasi-monodispersed Spherical TiO_2 Particles. *J. Inorg. Mater. Chin.* **2007**, *22*, 253–258.
38. Ma, L.M.; Zheng, F.X.; Zhao, X.P. Sedimentation behaviour of hierarchical porous TiO_2 microspheres electrorheological fluids. *J. Intel. Mater. Syst. Struct.* **2015**, *26*, 1936–1944. [CrossRef]
39. Wang, J.H.; Chen, G.W.; Yin, J.B.; Luo, C.R.; Zhao, X.P. Enhanced electrorheological performance and antisedimentation property of mesoporous anatase TiO_2 shell prepared by hydrothermal process. *Smart Mater. Struct.* **2017**, *26*, 035036. [CrossRef]
40. Wang, B.X.; Zhao, X.P. Core/Shell Nanocomposite Based on the Local Polarization and Its Electrorheological Behavior. *Langmuir* **2005**, *21*, 6553–6559. [CrossRef] [PubMed]
41. Yin, J.B.; Xia, X.; Wang, X.X.; Zhao, X.P. The electrorheological effect and dielectric properties of suspensions containing polyaniline@TiO_2 nanocable-like particles. *Soft Matter* **2011**, *7*, 10978–10986. [CrossRef]
42. Xiang, L.Q.; Zhao, X.P. Electrorheological activity of a composite of TiO_2-Coated Montmorillonite. *J. Mater. Chem.* **2003**, *13*, 1529–1532. [CrossRef]
43. Wang, B.X.; Zhao, X.P. Preparation of kaolinite/TiO_2 coated nanocomposite and their electro-rheological properties. *J. Mater. Chem.* **2003**, *13*, 2248–2253. [CrossRef]
44. Zhao, X.P.; Yin, J.B. Preparation and electrorheological characteristics of rare-earth-doped TiO_2 suspensions. *Chem. Mater.* **2002**, *14*, 2258–2263. [CrossRef]
45. Zhao, X.P.; Yin, J.B.; Xiang, L.Q.; Zhao, Q. Electrorheological fluids containing Ce-doped TiO_2. *J. Mater. Sci.* **2002**, *37*, 2569–2573. [CrossRef]
46. Zhao, X.P.; Yin, J.B.; Xiang, L.Q.; Zhao, Q. Effect of rare earth substitution on electrorheological properties of TiO_2. *Int. J. Mod. Phys. B* **2002**, *16*, 2371–2377. [CrossRef]
47. Yin, J.B.; Zhao, X.P. Temperature effect of rare earth-doped TiO_2 Electrorheological fluids. *J. Phys. D Appl. Phys.* **2001**, *34*, 2063–2067. [CrossRef]
48. Yin, J.B.; Zhao, X.P. Electrorheological effect of Cerium-Doped TiO_2. *Chin. Phys. Lett.* **2001**, *18*, 1144–1146.
49. Yin, J.B.; Zhao, X.P. Enhanced electrorheological activity of mesoporous Cr-doped TiO_2 from activated pore wall and high surface area. *J. Phys. Chem. B* **2006**, *110*, 12916–12925. [CrossRef] [PubMed]
50. Wang, B.X.; Zhao, X.P. A bionic nano-papilla particle and its super-oleophilic ability. *Adv. Funct. Mater.* **2005**, *15*, 1815–18212. [CrossRef]
51. Xiang, L.Q.; Zhao, X.P.; Yin, J.B. Micro/nano-structured montmorillonite/TiO_2 particles with high electrorheological activity. *Rheol. Acta* **2011**, *50*, 87–95. [CrossRef]
52. Qiao, Y.P.; Zhao, X.P.; Su, Y.Y. Dielectric metamaterial particles with enhanced efficiency of mechanical/electrical energy transformation. *J. Mater. Chem.* **2011**, *21*, 394–399. [CrossRef]
53. Eiden-Assmann, S.; Widoniak, J.; Maret, G. Synthesis and Characterization of Porous and Nonporous Monodisperse Colloidal TiO_2 Particles. *Chem. Mater.* **2004**, *16*, 6–11. [CrossRef]
54. Zhao, Y.; Jiang, L. Hollow Micro/Nanomaterials with Multilevel Interior Structures. *Adv. Mater.* **2009**, *21*, 3621–3638. [CrossRef]
55. Réti, B.; Kiss, G.I.; Gyulavári, T.; Baan, K.; Magyari, K.; Hernadi, K. Carbon sphere templates for TiO_2 hollow structures: Preparation, characterization and photocatalytic activity. *Catal. Today* **2017**, *284*, 160–168. [CrossRef]
56. Orellana, M.; Osiglio, L.; Arnal, P.M.; Pizzio, L.R. TiO_2 hollow spheres modified with tungstophosphoric acid with enhanced visible light absorption for the photodegradation of 4-chlorophenol. *Photochem. Photobiol. Sci.* **2017**, *16*, 46–52. [CrossRef] [PubMed]
57. Liu, Y.; Lan, K.; Bagabas, A.A.; Zhang, P.; Gao, W.; Wang, J.; Sun, Z.; Fan, J.; Elzatahry, A.A.; Zhao, D. Ordered Macro/Mesoporous TiO_2 Hollow Microspheres with Highly Crystalline Thin Shells for High-Efficiency Photoconversion. *Small* **2016**, *12*, 860–867. [CrossRef] [PubMed]
58. Li, Y.; Fu, Z.Y.; Su, B.L. Hierarchically Structured Porous Materials for Energy Conversion and Storage. *Adv. Funct. Mater.* **2012**, *22*, 4634–4667. [CrossRef]
59. Kim, Y.J.; Lee, M.H.; Kim, H.J.; Lim, G.; Choi, Y.S.; Park, N.G.; Kim, K.; Lee, W.I. Formation of Highly Efficient Dye-Sensitized Solar Cells by Hierarchical Pore Generation with Nanoporous TiO_2 Spheres. *Adv. Mater.* **2009**, *21*, 3668–3673. [CrossRef]
60. Ismail, A.A.; Bahnemann, D.W. mesoporous TiO_2 photocatalysts: Preparation, characterization and reaction mechanisms. *J. Mater. Chem.* **2011**, *21*, 11686–11707. [CrossRef]

61. Li, S.; Zheng, J.; Zhao, Y.; Liu, Y. Preparation of a three-dimensional ordered macroporous titanium dioxide material with polystyrene colloid crystal as a template. *J. Appl. Polym. Sci.* **2008**, *107*, 3903–3908. [CrossRef]
62. Hegazy, A.; Prouzet, E. Room temperature synthesis and thermal evolution of porous nanocrystalline TiO_2 anatase. *Chem. Mater.* **2012**, *24*, 245–254. [CrossRef]
63. Zheng, X.; Lv, Y.; Kuang, Q.; Zhu, Z.; Long, X.; Yang, S. Close-Packed Colloidal SiO_2 as a Nanoreactor: Generalized Synthesis of Metal Oxide Mesoporous Single Crystals and Mesocrystals. *Chem. Mater.* **2014**, *26*, 5700–5709. [CrossRef]
64. Yin, J.B.; Zhao, X.P. Preparation and Electrorheological Activity of Mesoporous Rare-Earth-Doped TiO_2. *Chem. Mater.* **2002**, *14*, 4633–4640. [CrossRef]
65. Yin, J.B.; Zhao, X.P. Wormhole-like mesoporous Ce-doped TiO_2: A new electrorheological material with high activity. *J. Mater. Chem.* **2003**, *13*, 689–695. [CrossRef]
66. Joo, J.B.; Lee, I.; Dahl, M.; Moon, G.D.; Zaera, F.; Yin, Y. Controllable Synthesis of Mesoporous TiO_2 Hollow Shells: Toward an Efficient Photocatalyst. *Adv. Funct. Mater.* **2013**, *23*, 4246–4254. [CrossRef]
67. Bian, Z.F.; Zhu, J.; Cao, F.L.; Huo, Y.N.; Lu, Y.F.; Li, H.X. Solvothermal synthesis of well-defined TiO_2 mesoporous nanotubes with enhanced photocatalytic activity. *Chem. Commun.* **2010**, *46*, 8451–8453. [CrossRef] [PubMed]
68. Seisenbaeva, G.A.; Moloney, M.P.; Tekoriute, R.; Hardy-Dessources, A.; Nedelec, J.M.; Gun'ko, Y.K.; Kessler, V.G. Biomimetic Synthesis of Hierarchically Porous Nanostructured Metal Oxide Microparticles-Potential Scaffolds for Drug Delivery and Catalysis. *Langmuir* **2010**, *26*, 9809–9817. [CrossRef] [PubMed]
69. Wang, C.; Yin, L.; Zhang, L.; Qi, Y.; Lun, N.; Liu, N. Large scale synthesis and gas-sensing properties of anatase TiO_2 Three-dimensional hierarchical nanostructures. *Langmuir* **2010**, *26*, 12841–12848. [CrossRef] [PubMed]
70. Rui, Y.; Wang, L.; Zhao, J.; Wang, H.; Li, Y.; Zhang, Q.; Xu, J. Template-free synthesis of hierarchical TiO_2 hollow microspheres as scattering layer for dye-sensitized solar cells. *Appl. Surf. Sci.* **2016**, *369*, 170–177. [CrossRef]
71. Zhang, D.; Li, G.; Wang, F.; Yu, J.C. Green synthesis of a self-assembled rutile mesocrystalline photocatalyst. *CrystEngComm* **2010**, *12*, 1759–1763. [CrossRef]
72. Liu, G.; Yang, H.G.; Sun, C.; Cheng, L.; Wang, L.; Lu, G.Q.; Cheng, H.M. Titania polymorphs derived from crystalline titanium diboride. *CrystEngComm* **2009**, *11*, 2677–2682. [CrossRef]
73. Yin, J.B.; Zhao, X.P.; Xiang, L.Q.; Xia, X.; Zhang, Z.S. Enhanced electrorheology of suspensions containing sea-urchin-like hierarchical Cr-doped TiO_2 particles. *Soft Matter* **2009**, *5*, 4687–4697. [CrossRef]
74. Vaneski, A.; Susha, A.S.; Rodríguez-Fernández, J.; Berr, M.; Jäckel, F.; Feldmann, J.; Rogach, A.L. Hybrid colloidal heterostructures of anisotropic semiconductor nanocrystals decorated with noble metals: Synthesis and function. *Adv. Funct. Mater.* **2011**, *21*, 1547–1556. [CrossRef]
75. Kochuveedu, S.T.; Kim, D.P.; Kim, D.H. Surface lasmon induced visible light photocatalytic activity of TiO_2 nanospheres decorated by Au nanoparticles with controlled configuration. *J. Phys. Chem. C* **2012**, *116*, 2500–2506. [CrossRef]
76. Grigorieva, A.V.; Goodilin, E.A.; Derlyukova, L.E.; Anufrieva, T.A.; Tarasov, A.B.; Dobrovolskii, Y.A.; Tretyakov, Y.D. TiO_2 nanotubes supported platinum catalyst in CO oxidation process. *Appl. Catal. A Gen.* **2009**, *362*, 20–25. [CrossRef]
77. Kafizas, A.; Dunnil, C.W.; Parkin, I.P. The relationship between photocatalytic activity and Photochromic state of nanoparticulate silver surface loaded titanium dioxide thin-films. *Phys. Chem. Chem. Phys.* **2011**, *13*, 13827–13838. [CrossRef] [PubMed]
78. Wodka, D.; Bielanska, E.; Socha, R.P.; Elzbieciak-Wodka, M.; Gurgul, J.; Nowak, P.; Warszynski, P.; Kumakiri, I. Photocatalytic activity of titanium dioxide modified by silver nanoparticles. *ACS Appl. Mater. Interfaces* **2010**, *2*, 1945–1953. [CrossRef] [PubMed]
79. Zhang, N.; Liu, S.; Fu, X.; Xu, Y.J. Selective Pt deposition onto the face (110) of TiO_2 assembled microspheres that substantially enhances the photocatalytic properties. *J. Phys. Chem. C* **2011**, *115*, 9136–9145. [CrossRef]
80. Feng, L.L.; Wu, X.C.; Ren, L.R.; Xiang, Y.J.; He, W.W.; Zhang, K.; Zhou, W.Y.; Xie, S.S. Well-controlled synthesis of Au@Pt nanostructures by gold-nanorod-seeded growth. *Chem. Eur. J.* **2008**, *14*, 9764–9771. [CrossRef] [PubMed]

81. Levin, C.S.; Hofmann, C.; Ali, T.A.; Kelly, A.T.; Morosan, E.; Nordlander, P.; Whitmire, K.H.; Halas, N.J. Magnetic-plasmonic core-shell nanoparticles. *J. Am. Chem. Soc.* **2009**, *3*, 1379–1388. [CrossRef] [PubMed]
82. Chen, L.Y.; Fujita, T.; Ding, Y.; Chen, M.W. A Three-dimensional gold-decorated nanoporous copper core-shell composite for electrocatalysis and nonenzymatic biosensing. *Adv. Funct. Mater.* **2010**, *20*, 2279–2285. [CrossRef]
83. Xuan, S.; Xiang, Y.; Wang, J.; Yu, J.C.; Leung, K.C. Preparation, Characterization, and Catalytic Activity of Core/Shell Fe_3O_4@Polyaniline@Au Nanocomposites. *Langmuir* **2009**, *25*, 11835–11843. [CrossRef] [PubMed]
84. Wang, L.; Clavero, C.; Huba, Z.; Carroll, K.J.; Carpenter, E.E.; Gu, D.F.; Lukaszew, R.A. Plasmonics and Enhanced Magneto-Optics in Core-Shell Co-Ag Nanoparticles. *Nano Lett.* **2011**, *11*, 1237–1240. [CrossRef] [PubMed]
85. Lu, Y.; Zhao, Y.; Yu, L.; Dong, L.; Shi, C.; Hu, M.J.; Xu, Y.J.; Wen, L.P.; Yu, S.H. Hydrophilic Co@Au Yolk/Shell Nanospheres: Synthesis, Assembly, and Application to Gene Delivery. *Adv. Mater.* **2010**, *22*, 1407–1411. [CrossRef] [PubMed]